JIPB Journal of Integrative Plant Biology

Research Article
https://doi.org/10.1111/jipb.13557

The transcription factor NAC102 confers cadmium tolerance by regulating *WAKL11* expression and cell wall pectin metabolism in *Arabidopsis*

Guang Hao Han[1†], Ru Nan Huang[1†], Li Hong Hong[1], Jia Xi Xu[1], Yi Guo Hong[1,2], Yu Huan Wu[1*] and Wei Wei Chen[1,3*]

1. Research Center for Plant RNA Signaling, College of Life and Environmental Sciences, Hangzhou Normal University, Hangzhou 310036, China
2. Warwick-Hangzhou RNA Signaling Joint Laboratory, School of Life Sciences, University of Warwick, Warwick CV4 7AL, United Kingdom
3. State Key Laboratory of Plant Physiology and Biochemistry, College of Life Sciences, Zhejiang University, Hangzhou 310058, China
†These authors contributed equally to this work.
*Correspondences: Yu Huan Wu (yuhuanwu@hznu.edu.cn); Wei Wei Chen (chenweiwei@hznu.edu.cn, Dr. Chen is fully responsible for the distribution of plant materials in this article)

Guang Hao Han

Wei Wei Chen

ABSTRACT

Cadmium (Cd) toxicity severely limits plant growth and development. Moreover, Cd accumulation in vegetables, fruits, and food crops poses health risks to animals and humans. Although the root cell wall has been implicated in Cd stress in plants, whether Cd binding by cell wall polysaccharides contributes to tolerance remains controversial, and the mechanism underlying transcriptional regulation of cell wall polysaccharide biosynthesis in response to Cd stress is unknown. Here, we functionally characterized an *Arabidopsis thaliana* NAC-type transcription factor, NAC102, revealing its role in Cd stress responses. Cd stress rapidly induced accumulation of *NAC102.1*, the major transcript encoding functional NAC102, especially in the root apex. Compared to wild type (WT) plants, a *nac102* mutant exhibited enhanced Cd sensitivity, whereas *NAC102.1*-overexpressing plants displayed the opposite phenotype. Furthermore, NAC102 localizes to the nucleus, binds directly to the promoter of *WALL-ASSOCIATED KINASE-LIKE PROTEIN11* (*WAKL11*), and induces transcription, thereby facilitating pectin degradation and decreasing Cd binding by pectin. Moreover, *WAKL11* overexpression restored Cd tolerance in *nac102* mutants to the WT levels, which was correlated with a lower pectin content and lower levels of pectin-bound Cd. Taken together, our work shows that the NAC102-WAKL11 module regulates cell wall pectin metabolism and Cd binding, thus conferring Cd tolerance in *Arabidopsis*.

Keywords: cadmium stress, cell wall, NAC102, transcriptional regulation, WAKL

Han, G.H., Huang, R.N., Hong, L.H., Xu, J.X., Hong, Y.G., Wu, Y.H., and Chen, W.W. (2023). The transcription factor NAC102 confers cadmium tolerance by regulating *WAKL11* expression and cell wall pectin metabolism in *Arabidopsis*. J. Integr. Plant Biol. **65:** 2262–2278.

INTRODUCTION

With the development of urbanization and industrialization, pollution by heavy metals (HMs) is becoming an increasingly serious environmental issue. Whereas some HMs, such as zinc (Zn), copper (Cu), and iron (Fe), are essential micronutrients for plants, others are non-essential and have deleterious effects on living organisms. This second group of HMs includes cadmium (Cd), which has no nutritional roles in plant growth or development. Rather, Cd adversely affects the uptake and transport of water and essential nutrients, the cell membrane system, antioxidant

enzyme systems, and photosynthesis; Cd also threatens the environment and human health via its accumulation in plant biomass and introduction into the food chain (Clemens et al., 2013; Shahid et al., 2017).

Plants have evolved multiple mechanisms to cope with Cd stress and other HM stresses (Hall, 2002; Shahid et al., 2017), such as secreting thiol-chelating compounds to sequester Cd outside the plant in the rhizosphere, sequestering Cd inside the plant in vacuoles, inhibiting Cd influx, promoting Cd efflux, and immobilizing Cd on cell walls. The plant cell wall primarily consists of pectin, hemicelluloses, and cellulose (Somerville et al., 2004), with pectin being the main component responsible for chelating metal cations (Willats et al., 2006). For this reason, fixation of HMs by cell walls has been proposed to protect sensitive sites in the protoplasm from HM toxicity, while forming a physical barrier to prevent HMs from entering the symplast.

Whether HM binding to the cell wall contributes to toxicity or to tolerance remains unclear. For instance, the binding of aluminum ions (Al^{3+}) to cell walls has long been proposed to contribute to tolerance of Al stress (Kochian, 1995). However, subsequent experimental evidence revealed that Al binding to the cell wall is instead responsible for Al toxicity (Yang et al., 2008, 2011). Similarly, lower and higher Cd fixation by the cell wall have each been reported to be associated with tolerance of Cd stress (Zhu et al., 2012, 2013; Shi et al., 2015; Hu et al., 2021; Liu et al., 2022). Roots with higher contents of the cell wall polymers suberin and lignin are more impermeable to Cd and therefore more resistant to Cd uptake and translocation into living tissues (Lux et al., 2011). Therefore, the role of cell walls in Cd stress responses remains an open question. Moreover, the mechanisms regulating the expression of cell-wall-related genes under Cd stress are unknown.

Various studies have shown that Cd-induced responses are initiated by transcriptional regulation. To date, many transcription factors (TFs), such as ETHYLENE RESPONSE FACTOR 104 (PvERF104) from the common bean (*Phaseolus vulgaris*) (Wang et al., 2023), WRKY13 (Sheng et al., 2019; Zhang et al., 2020), heat shock factor A4a (HsfA4a) (Shim et al., 2009), basic helix-loop-helix (bHLH) family members (Wu et al., 2012), ZAT6 (Chen et al., 2016), and MYB49 (Zhang et al., 2019), have been shown to confer tolerance of Cd exposure by modulating Cd-responsive gene expression.

NAC TFs are one of the largest TF families in plants, with crucial roles in development and in responses to environmental stresses (Puranik et al., 2012). Recently, several lines of evidence have suggested that NAC TFs participate in Cd stress responses in plants. For instance, three NAC TFs were identified as being responsive to Cd stress in *Aegilops markgrafii*, and individually overexpressing these TF genes increased Cd tolerance in transgenic wheat (*Triticum aestivum*) plants (Du et al., 2020). Similarly, expression of *OsNAC300*, a NAC TF gene in rice (*Oryza sativa*), was upregulated by Cd in a dose-dependent manner (Hu et al., 2021). Knockout of *OsNAC300* resulted in Cd sensitivity, whereas *OsNAC300* overexpression had opposite effects (Hu et al., 2021). Wang et al. (2020) also noted that OsSNAC1 controls Cd tolerance by regulating the expression of genes involved in mitogen-activated protein kinase (MAPK) signaling cascades. Recently, Meng et al. (2022) showed that NAC004 positively regulates Cd tolerance through increased Cd fixation by cell walls in *Arabidopsis*. However, it remains unclear how NAC004 regulates cell wall metabolism.

In this study, we used a reverse-genetics approach to identify genes participating in plant responses to Cd exposure. We identified an *Arabidopsis* NAC TF, NAC DOMAIN CONTAINING PROTEIN 102 (NAC102), that functions in Cd tolerance by modulating pectin metabolism in cell walls. Furthermore, we demonstrate that NAC102 can bind to the promoter of *CELL WALL-ASSOCIATED KINASE-LIKE PROTEIN11* (*WAKL11*) to regulate its expression under Cd stress.

RESULTS

NAC102 is implicated in Cd tolerance

To identify genes critical for Cd stress response, we used a reverse-genetics approach, screening *Arabidopsis* T-DNA insertion mutants for Cd sensitivity. We identified a mutant line, SALK_030702, which displayed significantly shorter primary roots and lower root biomass when grown on medium containing 50 μmol/L $CdCl_2$ compared to control conditions (Figure 1A–D). To test whether this T-DNA mutant line was sensitive to Cd, we grew Col-0 (wild type (WT)) and mutant seedlings hydroponically for 4 weeks in one-fifth strength Hoagland nutrient solution, before subjecting plants to the same nutrient solution alone (−Cd, control) or containing 30 μmol/L $CdCl_2$ (+Cd) for 4 d. In the absence of Cd, we observed no obvious differences between Col-0 and the mutant line SALK_030702 in terms of primary root length or fresh biomass of roots and shoots. By contrast, Cd-treated mutant plants had shorter primary roots and produced less biomass than WT, indicative of greater Cd sensitivity on the part of the mutant (Figure 1E–H).

Looking at public information available at the *Arabidopsis* Biological Resource Center (ABRC), we discovered that two T-DNA copies are inserted in the second exon of At5g63790, which encodes NAC102 (Figure S1A). We did not detect full-length transcripts for the major splice form *NAC102.1* in the SALK_030702 homozygous line (Figure S1B), indicating that *NAC102.1* is knocked out in this mutant (named *nac102* hereafter). Although At5g63790 is annotated as having two transcript isoforms, we determined that the abundance of *NAC102.1* (At5g63790.1) was about 480- and 25-fold higher than that of *NAC102.2* (At5g63790.2) in roots and shoots, respectively, by reverse transcription quantitative polymerase chain reaction (RT-qPCR) (Figure 1I, J). Moreover, *NAC102.1* transcripts were more abundant in roots than in shoots (Figure 1J). Therefore, we considered *NAC102.1* to be the major transcript isoform which encodes a functional NAC102.

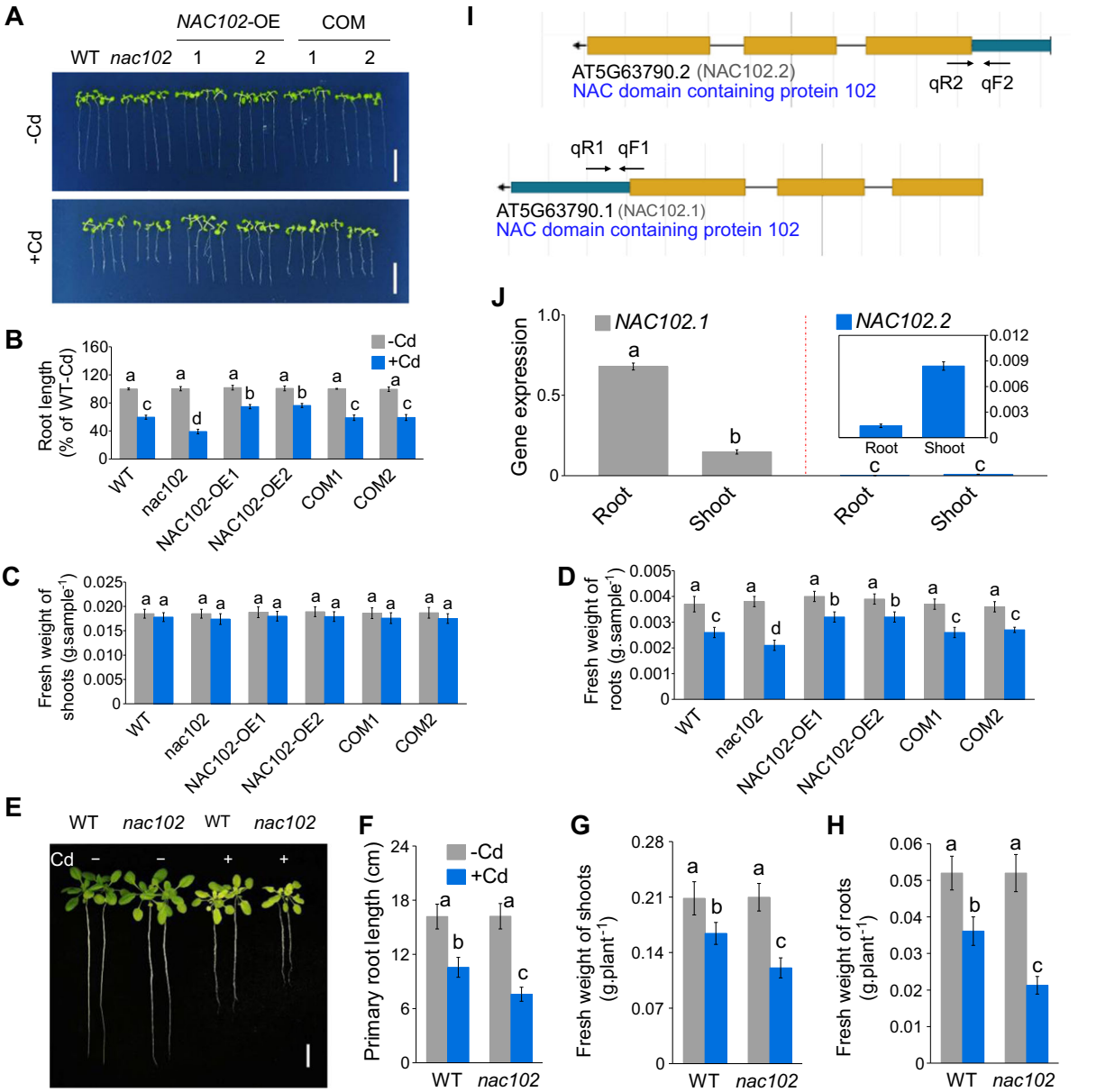

Figure 1. NAC102 is implicated in cadmium (Cd) resistance

(**A**–**D**) Cd sensitivity phenotypes (**A**), primary root growth (**B**), shoot fresh weight (**C**), and root fresh weight (**D**) under Cd stress. Seven-d-old seedlings of Col-0 plants (wild type (WT)), mutant *nac102* (SALK_030702), two independent *NAC102*-overexpressing lines (*NAC102*-OE1 and *NAC102*-OE2), and two independent complementation lines (COM1 and COM2) were transferred to 1/5 Hoagland solution supplied with either 0 or 50 μmol/L $CdCl_2$ for 4 d, then the phenotypes were photographed, and the length of primary roots was measured. For measurement of fresh weight of shoots and roots, 20 seedlings were collected as a sample, and then separated into shoots and roots. (**E**–**H**) Sensitive phenotype (**E**), root length (**F**), shoot fresh weight (**G**), and root fresh weight (**H**) of mutant *nac102* and WT under Cd stress. Four-week-old *Arabidopsis* seedlings of WT and mutant *nac102* were exposed to –Cd or +Cd medium for 4 d. (**I**) Schematic representation of two NAC102 transcripts, *NAC102.1* (AT5G63790.1) and *NAC102.2* (AT5G63790.2). The location of quantitative polymerase chain reaction primers used to distinguish the two NAC102 transcripts are shown. (**J**) Expression of *NAC102.1* and *NAC102.2* in roots and shoots of 7-d-old WT seedlings under normal conditions. The inset-figure, which has different y-axis scales, shows the low levels of *NAC102.2* messenger RNA in shoots. *ACTIN2* was used as internal control. Scale bars = 1 cm in panel (**A**), and 2 cm in panel (**C**). Data are means ± *SD* ($n = 20$ in panel (**B**), $n = 6$ in panels (**C, D**), $n = 7$ in panels (**F** – **H**), $n = 3$ in panel (**J**)), with different letters indicating significant differences among different treatments at $P \leq 0.05$.

To explore the contribution of NAC102 to Cd tolerance, we generated two complementation lines, named COM1 and COM2, in the *nac102* mutant background. Accordingly, we introduced the *NAC102.1pro::NAC102.1-GFP* transgene consisting of the *NAC102* promoter driving the expression of *NAC102* cloned in-frame and upstream of the sequence for green fluorescent protein (GFP) (Figure S1A–C). Under normal growth conditions (–Cd), we observed no significant differences in root elongation among WT, the *nac102* mutant, and the two COM lines. Under Cd stress, we measured close to a

70% inhibition in primary root elongation in *nac102*, but only 40% inhibition in WT and the COM lines (Figure 1A, B). This indicated that NAC102 is indeed responsible for the Cd sensitivity observed in the *nac102* mutant. We also generated two transgenic lines with stable *NAC102.1* overexpression (OE), named *NAC102*-OE1 and *NAC102*-OE2 (Figure S1A–C). We observed no differences in root growth under normal conditions between WT and these *NAC102*-OE lines; notably, the *NAC102*-OE lines had longer primary roots than WT upon Cd treatment (Figure 1A, B). These results implicated NAC102 in Cd tolerance in *Arabidopsis*.

NAC102 confers Cd tolerance by reducing root Cd accumulation

We examined the Cd contents of WT, the *nac102* mutant, the *NAC102*-OE lines, and the COM lines. In a first approach, we used the Cd-specific fluorescent probe Leadmium Green for visual observation of Cd accumulation in roots. In contrast to the low background green fluorescence seen in the absence of Cd, Leadmium Green signal strength dramatically increased after Cd treatment of WT and especially *nac102* mutant roots (Figure 2A). Quantification of fluorescence intensity confirmed the much higher signal in *nac102* compared to WT and the two COM lines, while revealing that the two *NAC102*-OE lines had the lowest fluorescence signal of all genotypes tested (Figure 2B).

In a complementary and more quantitative approach, we measured Cd content in 4-week-old plants by inductively coupled plasma optical emission spectroscopy (ICP-OES). Consistent with the fluorescence intensity obtained with Leadmium Green, the Cd content was highest in *nac102* mutant roots and lowest in the two *NAC102*-OE lines. Notably, most of the Cd accumulated in roots, accounting for more than 90% of total Cd content in these plants (Figure 2C), whereas we detected no significant difference in shoot Cd content among all genotypes (Figure 2D). We conclude that NAC102 appears to confer Cd tolerance by causing the accumulation of Cd in plant roots.

It has been suggested that the cell wall provides a physical barrier against Cd entry (Parrotta et al., 2015), which prompted us to measure the Cd contents in the root symplast versus apoplast. Consistent with the relatively high root total Cd content, Cd levels were much higher in the root apoplast than in the root symplast. When compared to WT and the COM lines, the *nac102* mutant accumulated more Cd in the apoplast and symplast than the other genotypes, whereas the two *NAC102*-OE lines exhibited the lowest Cd levels in both compartments (Figure 2E).

As *NAC102* expression levels were negatively correlated with Cd content, and although Cd contents were much higher in the apoplast than symplast, we investigated whether NAC102 regulated Cd accumulation mainly via the apoplast or symplast by carrying out a time-course experiment to analyze Cd accumulation in these two locations (Figure S2). We measured no difference in symplastic Cd content among the different genotypes tested (*nac102*, WT, *NAC102*-OE) over 3 d of Cd treatment; however, apoplastic Cd content was higher in the *nac102* mutant than in WT plants on the first day, and the difference became more pronounced over time. By the second day of Cd treatment, the two *NAC102*-OE lines displayed significantly less apoplastic Cd accumulation than WT. Thus, NAC102 preferentially affects apoplastic Cd accumulation in *Arabidopsis* roots.

Cell wall pectin confers NAC102-mediated Cd tolerance

The increased accumulation of Cd in the root apoplast prompted us to investigate the composition of cell wall polysaccharides, which have been reported to be associated with Cd tolerance (Meng et al., 2022). Although we observed no differences in root pectin content among genotypes in the absence of Cd, we noted a significant increase in root pectin content for all genotypes upon Cd stress, with the *nac102* mutant accumulating 35% more pectin than WT, whereas the two *NAC102*-OE lines had the lowest pectin levels among all genotypes (Figure 3A). We detected no difference in hemicellulose 1 (HC1), HC2, or cellulose contents in the roots of any genotype regardless of Cd status (Figures 3B, 3C, S3A). Moreover, more root cell wall pectin accumulated at increasing Cd concentrations (Figure S4), suggesting that root pectin accumulation is affected by Cd stress. Notably, Cd content in different cell wall fractions was consistent with their polysaccharide contents. In the pectin fraction, Cd content was highest in the *nac102* mutant, lower in WT and the COM lines, and lowest in the two *NAC102*-OE lines (Figure 3D). In the HC1 and HC2 fractions, we detected no difference in Cd content among the genotypes (Figure 3E, F); we also did not detect any Cd in the cellulose fraction for any genotype tested (Figure S3B).

NAC102.1 is induced by Cd stress in roots but not in shoots

To examine the tissue-specific expression pattern of *NAC102.1*, we generated *NAC102.1pro::GUS* reporter lines by placing the *NAC102* promoter (upstream of the *NAC102.1* translational start site) upstream of the β-glucuronidase (*GUS*) reporter gene. At the seedling stage, we detected GUS signals in roots but almost none in the hypocotyl or cotyledons (Figure 4A), which was consistent with our RT-qPCR analysis showing *NAC102.1* expression mainly in roots (Figure 1J). Exposure to Cd resulted in stronger GUS signals in roots but not in aerial tissues (Figure 4B). In the absence of Cd, GUS activity was strong in the root tip but very weak at the root apical meristem, whereas Cd stress dramatically enhanced GUS activity throughout the entire root (Figure 4A–D). At the reproductive stage, GUS signals were detected from the *NAC102.1pro::GUS* reporter assay in roots, rosette leaves, cauline leaves, and flowers, but not in siliques (Figure S5A–E). In agreement with this, RT-qPCR analysis showed that *NAC102.1* was constitutively expressed in the roots, leaves, and flowers of 6-week-old WT plants (Figure S5F).

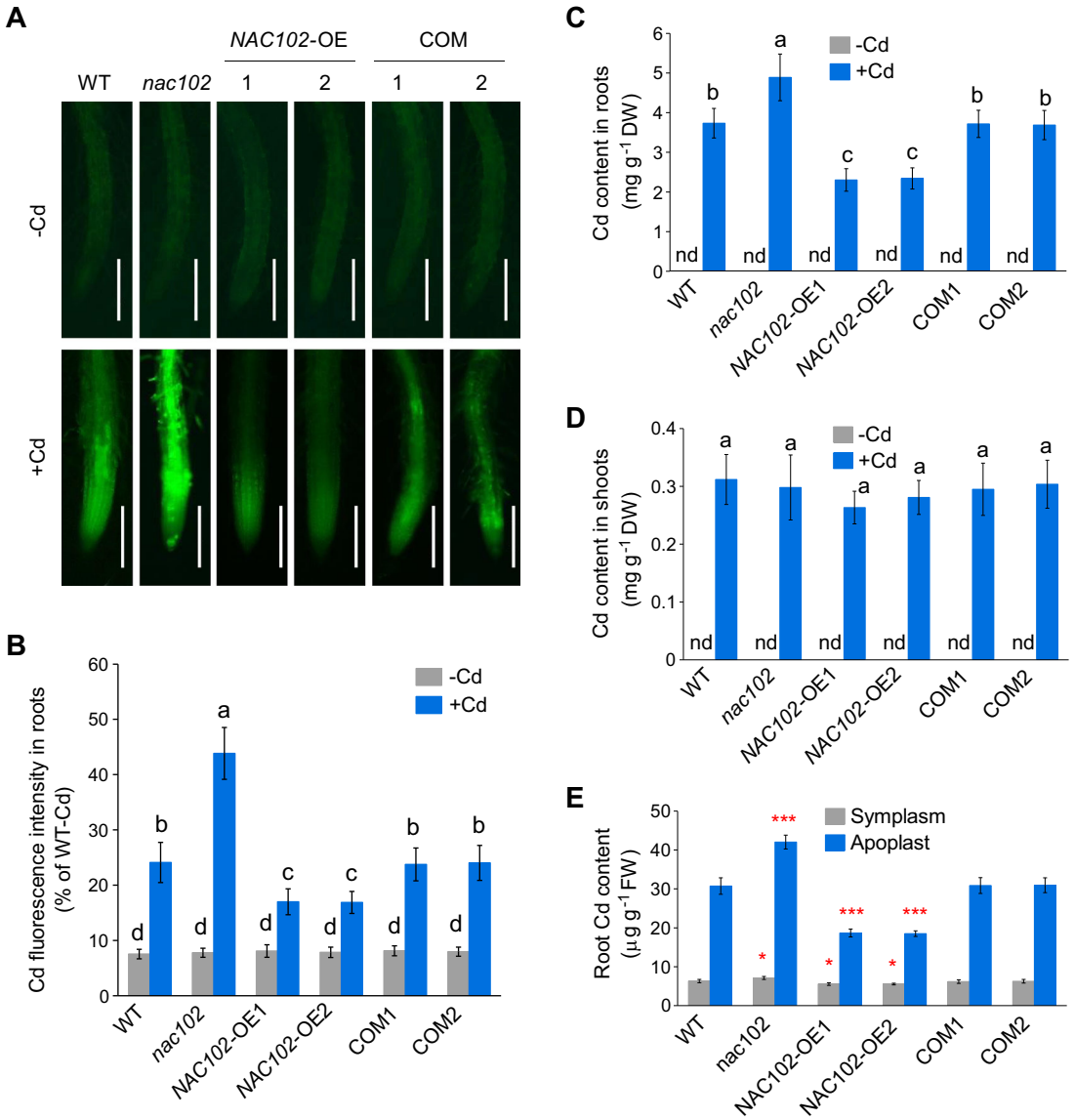

Figure 2. Mutation of *NAC102.1* results in cadmium (Cd) accumulation in roots

(**A, B**) Cd-specific fluorescence (**A**) and the relative signal intensity (**B**) in roots under Cd stress. Seven-d-old seedlings of wild type (WT), mutant *nac102*, *NAC102*-OE (overexpression) lines and complementation (COM) lines with 1-cm root length were exposed to 1/5 Hoagland solution containing 50 μmol/L $CdCl_2$ for 4 d. The Cd-specific fluorescence probe, Leadmium Green, was used to detect the distribution of Cd in roots. Scale bars = 200 μm in panel (**A**). (**C, D**) Cd content in roots (**C**) and shoots (**D**). (**E**) Symplastic and apoplastic Cd content in roots. Four-week-old seedlings of WT, mutant *nac102*, *NAC102*-OE lines and COM lines were transferred to –Cd or +Cd conditions. After a 4-d treatment, roots and shoots were harvested for Cd analysis by inductively coupled plasma optical emission spectroscopy (ICP-OES). Means ± *SD* ($n = 10$ for Cd fluorescence intensity, $n = 6$ for Cd content). In panels (**C, D**), n.d. indicates that the Cd content was almost undetectable in roots or shoots under normal conditions among all genotypes tested; in panels (**B**–**D**), different letters indicate significant differences among treatments at $P \leq 0.05$, while in panel (**E**), asterisks indicate significant differences compared to the WT control (*$P \leq 0.05$; **$P \leq 0.01$; ***$P \leq 0.001$).

Since the transcript abundance of *NAC102.1* increased at least two-fold in response to Cd stress (Figure S6), we examined whether the abundance of NAC102 protein changed in response to Cd exposure. Using the COM lines harboring the *NAC102.1pro::NAC102.1-GFP* transgene, we evaluated NAC102 protein by detecting GFP signals in roots. Consistent with the GUS assays, almost no GFP signal was detectable under normal conditions, but we observed rapid accumulation of GFP signals within the nucleus following Cd treatment (Figure 4E).

We dissected the transcriptional regulation of *NAC102.1* by Cd stress through a time-course experiment in which we transferred seedlings to medium containing 30 μmol/L Cd; this revealed that *NAC102.1* expression was induced after 1 h of exposure, with a peak at 24 h of exposure followed by a subsequent drop (Figure 4F). However, relative *NAC102.1* transcript levels remained higher 96 h into Cd treatment compared to those at the 0-h time point. A dose-dependent experiment showed a gradual rise in *NAC102.1* transcript

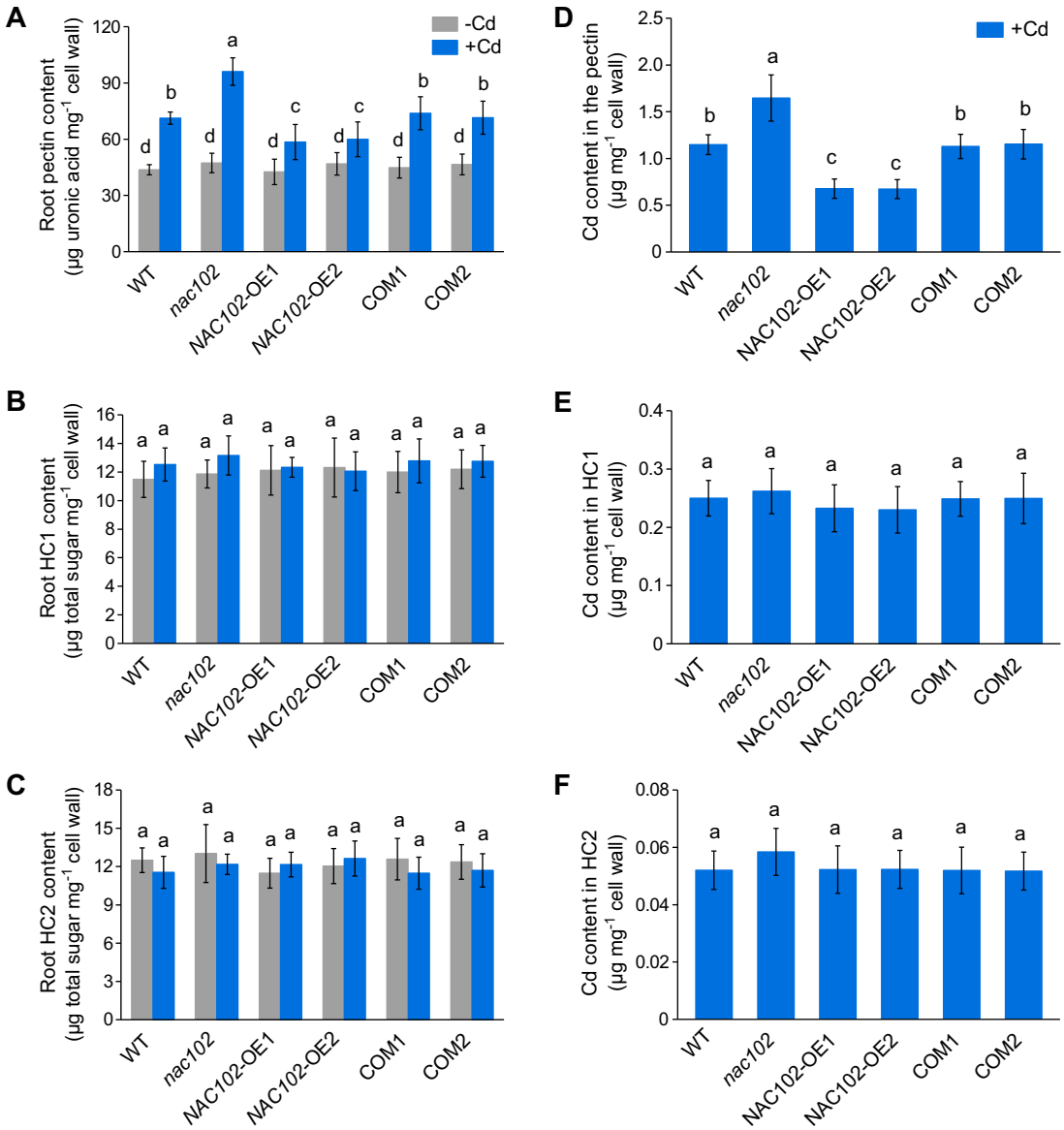

Figure 3. Cell wall pectin contributes to NAC102.1-mediated cadmium (Cd) tolerance

(**A**–**C**) Pectin content (**A**), hemicellulose 1 (HC1) content (**B**), and hemicellulose 2 (HC2) content (**C**) in the cell wall of roots under Cd stress. (**D**–**F**) Cd content in the pectin (**D**), HC1 (**E**), and HC2 (**F**) under Cd stress. Four-week-old seedlings of wild type (WT), mutant *nac102*, *NAC102*-OE (overexpression) lines and (complementation) COM lines were grown under −Cd or +Cd conditions for 4 d. Data are means ± *SD* ($n = 6$). Bars with different letters are significantly different among genotypes at the level of $P \leq 0.05$.

abundance with increasing Cd concentrations (Figure 4G). These results indicate that NAC102 functions positively to regulate Cd stress responses in roots.

Nucleus-localized NAC102 binds to the *WAKL11* promoter and activates its transcription

We investigated the subcellular localization of NAC102 by transiently expressing the *35S::NAC102.1-GFP* construct in *Nicotiana benthamiana* leaves together with the nuclear marker construct *H2B-RFP*, encoding histone H2B fused to red fluorescent protein (RFP). The fluorescence signals from NAC102-GFP largely overlapped with those of H2B-RFP (Figure 5A). We introduced the same *35S::NAC102.1-GFP* construct into Col-0 and obtained stable transgenic lines; in the root tips of the resulting seedlings, we observed substantial overlap between GFP fluorescence and 4′,6-diamidino-2-phenylindole (DAPI) signals in the nucleus (Figure 5B).

We also assessed the transactivation potential of NAC102 in a yeast expression system. We divided the predicted NAC102 protein into different fragments based on its functional domains, and cloned each encoding fragment in-frame with a plasmid carrying the sequence encoding the DNA-binding domain of the yeast (*Saccharomyces cerevisiae*)

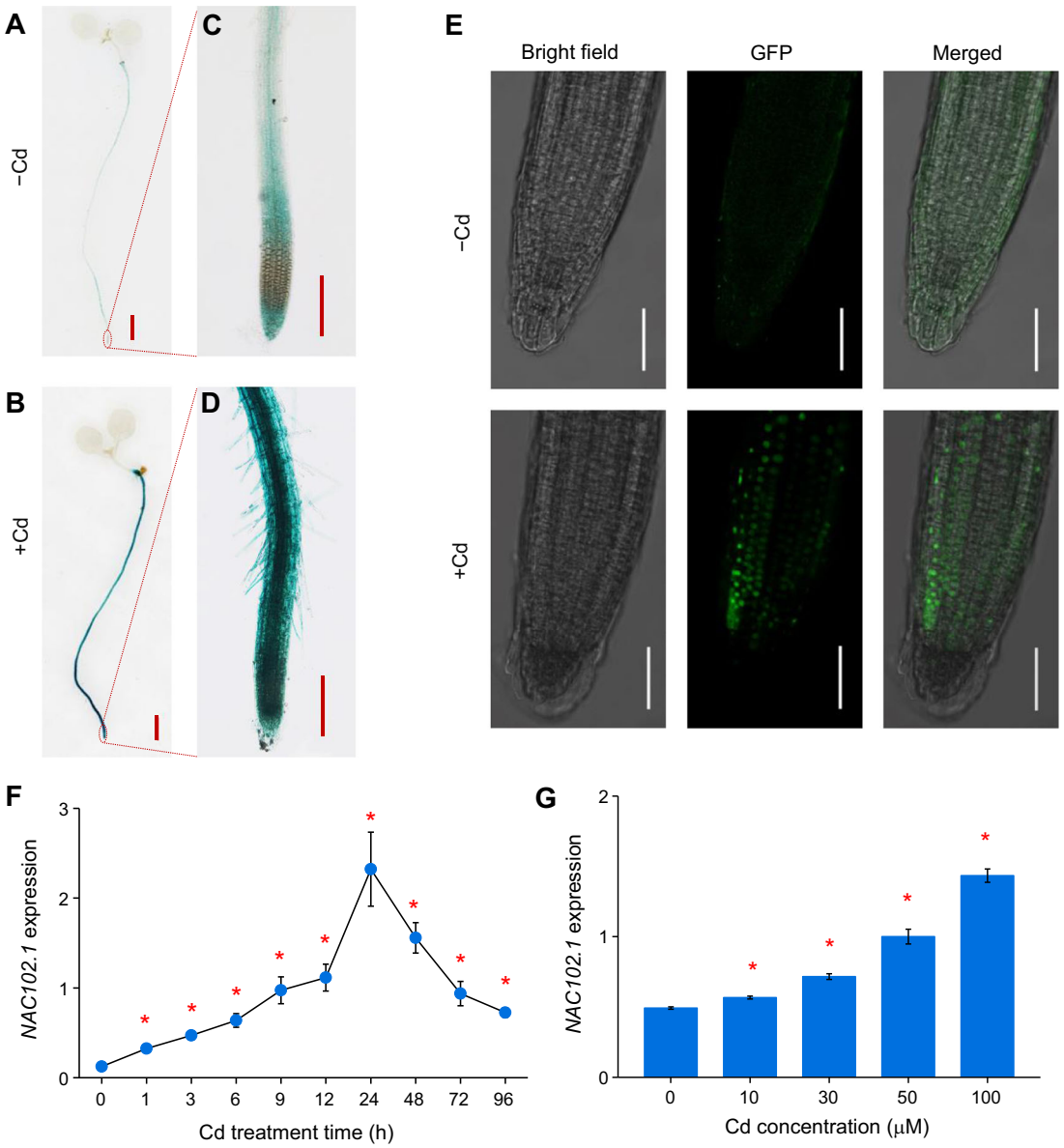

Figure 4. Expression pattern of *NAC102.1* under cadmium) Cd stress

(**A**–**D**) *NAC102.1pro::GUS* expression analysis in the whole seedlings (**A, B**) and root apex (**C, D**). Transgenic *Arabidopsis* seedlings at 7-d-old were exposed to 0 or 50 μmol/L $CdCl_2$ for 24 h. Scale bars = 1 mm in panels (**A, B**); 200 μm in panels (**C, D**). (**E**) Accumulation of NAC102 protein by detecting green fluorescence signals induced by Cd stress. Seven-d-old complementation (COM) lines (*nac102 NAC102.1pro::NAC102.1-GFP*) were treated with 0 or 50 μmol/L $CdCl_2$ for 10 min, and then the fluorescence signals of NAC102-GFP (green fluorescent protein) fusion protein were analyzed. GFP: GFP fluorescence; Merged: GFP/bright field overlay. Scale bars = 50 μm. (**F**) Time-dependent expression of *NAC102.1* in roots responding to Cd stress for different times. Four-week-old seedlings of wild type (WT) were grown under +Cd conditions for 0, 1, 3, 6, 9, 12, 24, 48, 72, and 96 h. (**G**) Dose-response of *NAC102.1* in *Arabidopsis* root under Cd stress. Four-week-old seedlings of WT were exposed to 0, 10, 30, 50, and 100 μmol/L $CdCl_2$ for 96 h. Data are means ± *SD* (*n* = 3 of biological repeats). *ACTIN2* was used as internal control. Asterisks are significantly different compared to the 0 h or 0 μmol/L control at $P \leq 0.05$.

GAL4 TF, before transforming the resulting constructs individually into yeast AH109. Yeast cells carrying BDGAL4-NAC102 (amino acids (aa) 1 – 313), BDGAL4-NAC102 (aa 51 – 313), and BDGAL4-NAC102 (aa 175 – 313) grew well on synthetic defined (SD) medium lacking histidine, while cells carrying BDGAL4 alone, BDGAL4-NAC102 (aa 1 – 50), BDGAL4-NAC102 (aa 51 – 174), and BDGAL4-NAC102 (aa 1 – 174) did not (Figure 5C). These results indicate that NAC102 is a nuclear protein with a transactivation domain located in its C-terminal region (aa 175 – 313).

Our previous study showed that NAC-type aluminum responsive 1 (VuNAR1), a NAC TF in rice bean (*Vigna umbellata*), regulates *VuWAK1* expression, which contributes to cell wall pectin metabolism and Al binding capacity (Lou et al., 2019). Wall-associated kinases (WAKs), or WAK-like kinases (WAKLs), are receptor-like kinases attached to cell wall pectin

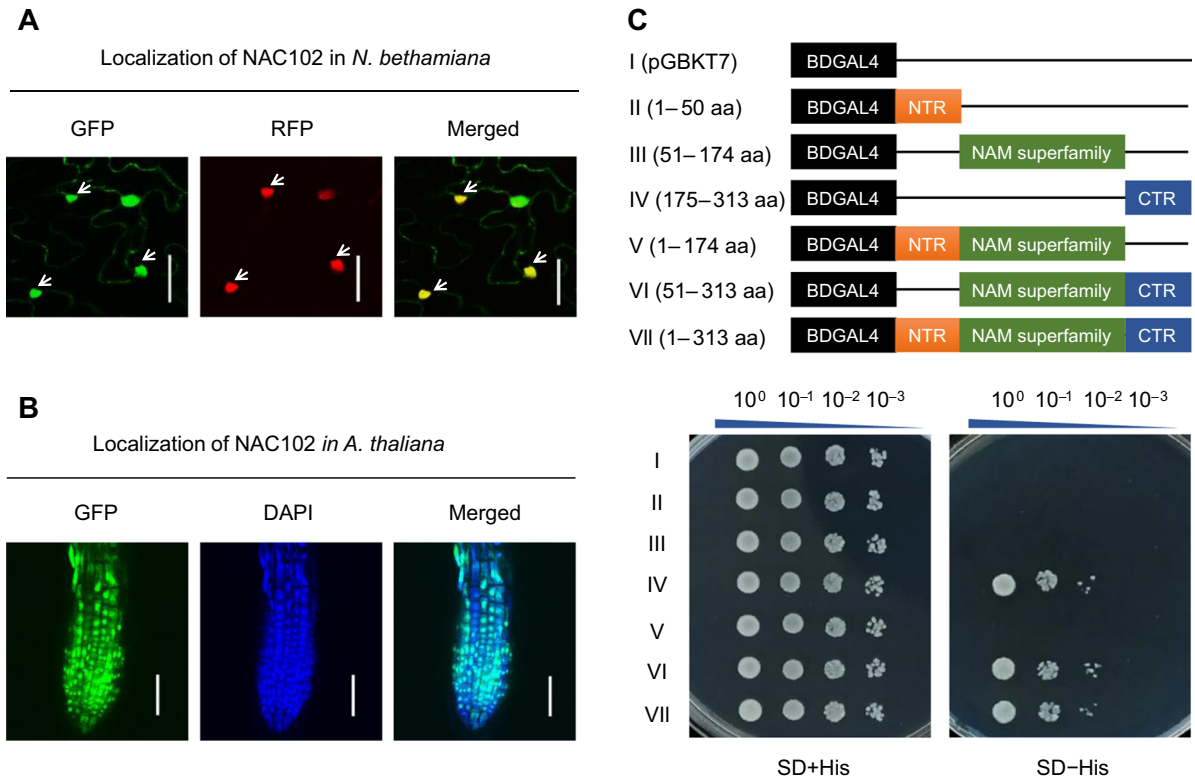

Figure 5. Nucleus-localized NAC102 has transactivation potential

(**A, B**) Subcellular localization. The *35S::NAC102.1-GFP* (green fluorescent protein) construct was transiently expressed in *Nicotiana benthamiana* leaves with the nuclear marker histone H2B-RFP (red fluorescent protein) (**A**), or constitutively expressed in transgenic *Arabidopsis* plants with 4′,6-diamidino-2-phenylindole (DAPI) signals along the primary root (**B**). White arrowheads indicate nuclei. DAPI, DAPI fluorescence; GFP, GFP fluorescence; RFP, red fluorescent protein fluorescence; Merged: GFP/RFP or GFP/DAPI field overlay. Scale bars = 50 μm. (**C**) Transcriptional activation assay. The full-length amino acid sequence of NAC102.1 was truncated to generate six fragments including that encoded by the full-length complementary DNA (II-VII), in which the empty pGBKT7 vector was used as the control (I). The recombinant vectors were introduced individually into yeast strain *AH109* (carrying the GAL4-responsive GAL1 promoter and the HIS3 reporter gene), and cultured on synthetic defined medium without His at 30°C for 3 d. NTR: N-terminal region; NAM family: NAC domain; CTR: C-terminal region.

with a cytoplasmic protein kinase domain (Verica and He, 2002; Lou et al., 2019). We therefore tested whether NAC102 might affect pectin content and Cd accumulation in roots by regulating expression of *WAK* or *WAKL* genes. Notably, among the five *WAK* and 22 *WAKL* genes in the *Arabidopsis thaliana* genome (Verica and He, 2002), an RT-qPCR analysis determined that the expression of *WAKL11* is upregulated by Cd stress in WT, and this induction was abolished in the *nac102* mutant (Table S1). In agreement with the RT-qPCR results, Cd treatment enhanced root GUS activity in *WAKL11pro::GUS* reporter lines, but this enhancement was less pronounced in *nac102 WAKL11pro::GUS* reporter lines (Figure 6A). Notably, the expression of *WAKL11* in *NAC102*-OE lines was higher under Cd stress conditions (Table S1). These results suggest that the transcriptional induction of *WAKL11* by NAC102 occurs under Cd stress.

To examine whether NAC102 binds to the *WAKL11* promoter, we conducted a yeast one-hybrid assay. We divided the 2,022-bp promoter region of *WAKL11* into nine fragments, A1 to A9 (Figure 6B). NAC TFs have been reported to recognize DNA sequences containing CGT(G/A) or CATG motifs (Simpson et al., 2003; Tran et al., 2004). Our search for such *cis*-acting elements identified CGTG motifs in A1, A2, and A3 but not in the other fragments. Notably, NAC102 strongly bound to A1, but not A2 or A3, in the yeast one-hybrid assay. Additionally, NAC102 also bound to the A5, A6, and A7 fragments, which lack a CGTG *cis*-element, suggesting that these fragments may contain other binding motifs (Figure 6C).

To independently test the binding of NAC102 to the *WAKL11* promoter, we performed chromatin immunoprecipitation followed by qPCR (ChIP-qPCR), using an anti-GFP antibody and Cd-treated COM transgenic lines. ChIP-qPCR revealed relative enrichment of *WAKL11* promoter fragments A1 and A7 of 5.5- and 1.6-fold, respectively, compared to WT plants; however, we detected no enrichment of the A5 and A6 fragments in the precipitated chromatin (Figure 6D). As an independent *in vivo* confirmation of the interaction between NAC102 and the *WAKL11* promoter, we performed a transient firefly luciferase (*LUC*) reporter assay, whereby we placed *LUC* under the control of each of the four above promoter fragments and co-infiltrated each *LUC* construct into *N. benthamiana* together with the *NAC102* effector construct (Figure 6E). We detected no LUC

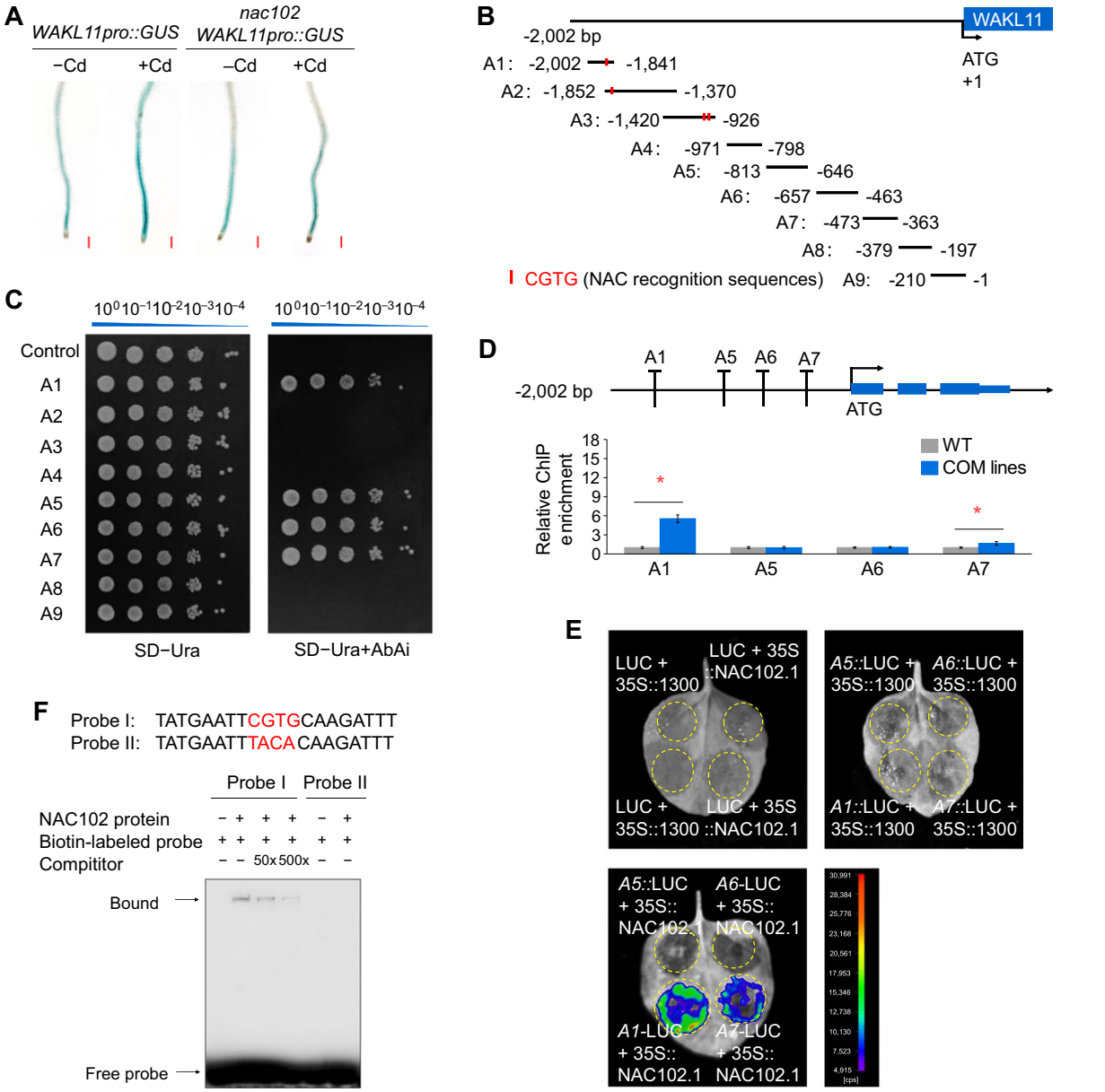

Figure 6. NAC102 activates *CELL WALL-ASSOCIATED KINASE-LIKE PROTEIN11* (*WAKL11*) transcription by directly binding to its promoter

(**A**) *WAKL11pro::GUS* expression analysis in roots of transgenic *Arabidopsis* plants. Seven-d-old transgenic seedlings of *WAKL11pro::GUS* and *nac102 WAKL11pro::GUS* were exposed to –Cd or +Cd media for 24 h. Scale bars = 200 μm. (**B**) Schematic representation showing the *WAKL11* promoter fragments (A1 – A9) used to construct the reporter vectors for yeast one-hybrid (Y1H) assay. The locations of known NAC binding *cis*-elements in the *WAKL11* promoter are marked. (**C**) Y1H analysis. A pair of plasmids, pAbAi-*WAKL11pro* and pGADT7-NAC102.1, were introduced into yeast strain *Y1HGold* and cultured on synthetic defined (SD) medium without Ura but containing 200 ng/mL AbAi. (**D**) Schematic representation showing the genomic structure of *WAKL11*, and chromatin immunoprecipitation – quantitative polymerase chain reaction (ChIP-qPCR) analysis of NAC102 binding to the promoter regions of *WAKL11*. Four-week-old seedlings of wild type (WT) and complementation (COM) (*nac102 NAC102.1pro::NAC102.1-GFP*) transgenic plants were exposed to +Cd media for 24 h, and then used for chromatin DNA isolation, which was then immunoprecipitated with anti-GFP (green fluorescent protein) antibody. The promoter fragments, A1, A5, A6, and A7, were the same as shown above. qPCR was performed to detect the enrichment of *WAKL11* promoter fragments in the immunoprecipitant, and fold enrichment indicates the immunoprecipitation efficiency in the transgenic plants normalized to that in WT plants. Asterisks indicate significant differences versus WT plants ($P \leq 0.05$). (**E**) Transient transcriptional activity assay. The *WAKL11* promoter fragments A1, A5, A6 and A7 were separately cloned into pGreenII0800-LUC (a luciferase (LUC)-based reporter vector driven by 35S mini promotor), and the coding sequence of *NAC102.1* was cloned into 35S::pCAMBIA1300. The recombinant constructs were transiently co-expressed in *Nicotiana benthamiana* leaves via Agroinfiltration, and the luminescence intensity (counts per second) is indicated by the colored scale bars. (**F**) Electrophoretic mobility shift assay. Two single-stranded biotin-labeled oligonucleotide probes were synthesized containing CGTG motif, or mutated TACA motif. Unlabeled DNA fragments were used as competitors. The NAC102 protein was extracted from *35S::NAC102-GFP* transgenic plants with stably expressing NAC102-GFP fusion proteins.

signal from leaves infiltrated with the *LUC* reporter or the effector construct alone. By contrast, leaves co-infiltrated with *NAC102* and *A1::LUC* or *NAC102* and *A7::LUC* displayed strong luminescence signals, suggesting that NAC102 directly activates *WAKL11* transcription, especially by binding to the A1 fragment *in planta*.

Finally, to assess the binding efficiency of NAC102 to the *WAKL11* promoter, we performed an electrophoretic mobility shift assay (EMSA), starting by immune purifying NAC102-GFP from transgenic *35S::NAC102.-GFP* plants using an anti-GFP antibody, in which we detected a clear band of the appropriate molecular weight corresponding to the NAC102-GFP fusion protein (Figure S7). We then mixed the purified protein with biotin-labeled probe I (positive control, −1,869 bp to −1,850 bp counting from the translational start codon and containing the GTCT motif) (Figure 6F, top); we determined that probe I binds to NAC102-GFP. This binding was completed by the addition of excess non-biotin-labeled probe I to the reaction (Figure 6F, bottom). Importantly, biotin-labeled probe II, the mutated version of probe I, showed no binding to NAC102 (Figure 6F).

WAKL11 is epistatic to NAC102 in regulating Cd tolerance

As *WAKL11* is a putative downstream target gene of NAC102, we evaluated the role of *WAKL11* in Cd tolerance. To this end, we generated three knockout mutants for *WAKL11* by clustered regularly interspaced short palindromic repeat (CRISPR)/CRISPR-associated nuclease 9 (Cas9)-mediated-editing and named these mutants *wakl11-1*, *wakl11-2* and *wakl11-3* (Figure S8A). We also produced transgenic lines overexpressing *WAKL11* and chose three independent lines with *WAKL11* expression levels about 60-fold higher than WT: *WAKL11*-OE1, *WAKL11*-OE2, and *WAKL11*-OE3 (Figure S8B). Whereas all three *wakl11* mutants displayed reduced primary root elongation, *WAKL11*-OE lines had the opposite phenotype (Figure S8C, D). Given that we attributed the changes of pectin content and Cd accumulation in the *nac102* mutant to the loss of *WAKL11* expression (Figures 3, 6), we hypothesized that the changes in pectin and Cd accumulation reflected changes in *WAKL11* expression. Indeed, the pectin content in roots was higher in the *wakl11* mutants but lower in *WAKL11*-OE lines compared to WT plants (Figure S8E). Neither HC1 nor HC2 content were affected by *WAKL11* (Figure S8F, G). We detected more Cd accumulating in the pectin of *wakl11* mutants but less in *WAKL11*-OE lines, with no differences in Cd contents in the HC1 or HC2 fractions (Figure S8H–J).

To provide genetic evidence that WAKL11 is epistatic to NAC102, we generated the genotypes *wakl11 nac102* (using all three available *wakl11* alleles) and *nac102 WAKL11*-OE (with all three *WAKL11*-OE lines) by genetic crossing. The *wakl11 nac102* double mutants exhibited the same Cd sensitivity as the *nac102* mutant, and thus were more sensitive than WT plants. However, when *WAKL11* was overexpressed in the *nac102* background, the sensitivity of the resulting *nac102* *WAKL11*-OE lines returned to WT levels (Figure 7A, B), implying that WAKL11 acts downstream of NAC102 to modulate Cd tolerance. Consistent with this, the pectin content of roots and its bound Cd content were comparable between the *nac102* and *wakl11 nac102* mutants, but they were higher than those of WT exposed to Cd (Figure 7C, D). By contrast, pectin content and its Cd content did differ between WT and *nac102* *WAKL11*-OE lines (Figure 7C, D), but the hemicellulose content or its bound Cd content did not differ among the different genotypes (Figure S9).

DISCUSSION

NACs are plant-specific TFs that play vital roles during plant growth and stress responses (Jin et al., 2022). NAC102 was previously reported to be responsive to waterlogging-induced oxygen deficiency and high light intensity (Christianson et al., 2009). Excessive light leads to the accumulation of peroxides and other toxic metabolites, which trigger the SCARECROW-LIKE 14 (SCL14)-dependent expression of *NAC102* to regulate the expression of many genes encoding detoxification enzymes (D'Alessandro et al., 2018).

NAC102 was also reported to be involved in brassinosteroid homeostasis. By interacting with ATAF1, ATAF2, and CIRCADIAN CLOCK ASSOCIATED 1 (CCA1), NAC102 regulates the expression of two genes encoding cytochrome P450 enzymes, BAS1 (PHYB ACTIVATION TAGGED SUPPRESSOR 1) and SOB7 (SUPPRESSOR of *phyB-4* 7), leading to brassinosteroid catabolism (Peng and Neff, 2021). Exogenous treatment with brassinolide downregulates *NAC102* expression, and the *nac102* mutant is partially insensitive to brassinolide (Peng and Neff, 2021).

In this study, we propose that NAC102 modulates Cd tolerance in *Arabidopsis*. First, *NAC102.1*, the major transcript that encodes the functional NAC102 protein (Figure 1I, J), was rapidly induced by Cd (Figure 4), especially at the root apex (Figure 4D), which plays an important role in regulating cell division and elongation, as well in the uptake of water and nutrients (Kong et al., 2018). Second, loss-of-function mutation of *NAC102* resulted in greater sensitivity to Cd stress (Figure 1A–H), whereas overexpression of *NAC102.1* had the opposite effect (Figure 1A–D).

Indeed, we demonstrated that NAC102 regulates Cd tolerance by affecting cell wall pectin metabolism; this is supported by the following lines of evidence. First, apoplastic Cd preferentially accumulated in all genotypes, but especially in the *nac102* mutant (Figures 2E, S2), and the roots of the *nac102* mutant retained more apoplastic Cd in their cell wall pectin (Figure 3), suggesting that NAC102 plays an important role in regulating apoplastic Cd retention. Second, the rescue of the Cd sensitivity of the *nac102* mutant seen in complementation lines was accompanied by lower Cd accumulation in the root apoplast and lower cell wall pectin content, resulting in lower Cd accumulation in pectin (Figures 2E, S2). Conversely, overexpression of *NAC102.1* resulted in lower

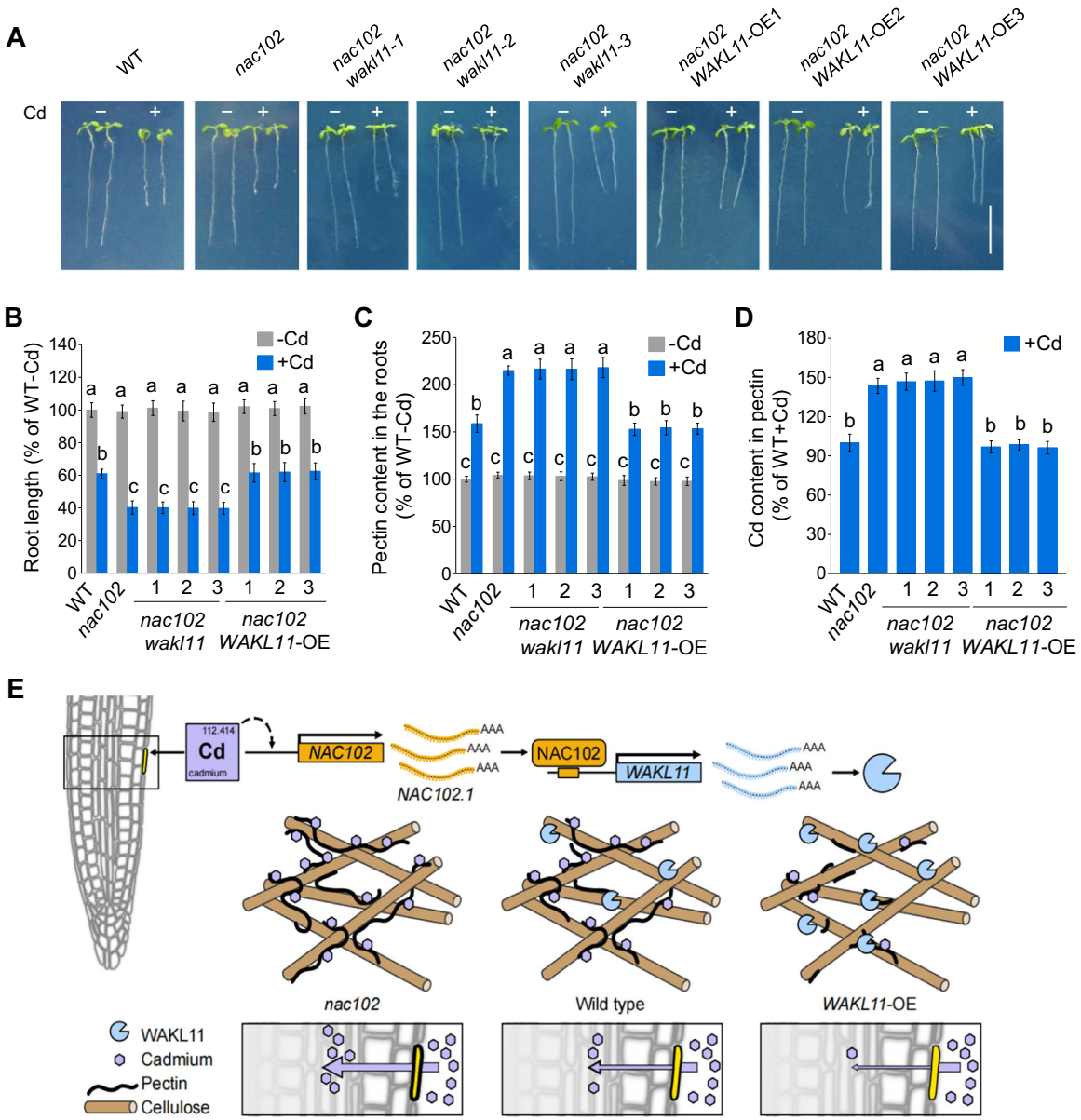

Figure 7. CELL WALL-ASSOCIATED KINASE-LIKE PROTEIN11 (WAKL11) is involved in NAC102-mediated cadmium (Cd) resistance

(**A, B**) Cd sensitivity phenotypes (A) and relative root elongation (B) of wild type (WT) plants, *nac102* mutant and three independent lines of *nac102 wakl11* double mutants and *nac102 WAKL11*-OE (overexpression) lines. Seven-d-old seedlings with 1-cm root length were treated with 0 or 50 μmol/L $CdCl_2$ for 4 d. Scale bars = 1 cm in panel (**A**). (**C, D**) Cell wall pectin content and its Cd retention in roots of *nac102 wakl11* double mutants and *nac102 WAKL11*-OE lines. Four-week-old seedlings were treated under −Cd or +Cd conditions for 4 d. Data are normalized to that of WT under −Cd conditions (WT−Cd). Means ± *SD* ($n = 20$ for primary root growth, $n = 8$ for pectin and Cd content) with different letters indicating significantly differences among genotypes with or without Cd treatment at $P \leq 0.05$. (**E**) Working model for the role of NAC102–WAKL11 module in regulating Cd stress responses in *Arabidopsis*. Under Cd stress, *NAC102.1* transcript is induced and encodes the functional NAC102 proteins, which are able to bind directly to the promoter of *WAKL11* to activate its expression. The increased expression of *WAKL11* contributes to cell wall pectin degradation, thereby decreasing Cd accumulation in roots and conferring Cd resistance. Note that since hemicellulose does not appear to be involved in Cd tolerance, it is not being represented in the working model for clarity.

pectin content and diminished Cd accumulation (Figure 3). These results suggest that NAC102 regulates apoplast Cd accumulation by affecting cell wall pectin metabolism. Third, the relative transcript level of *WAKL11* rose under Cd stress, but this induction was largely blocked in the *nac102* mutant (Figure 6A; Table S1), indicating that NAC102 acts upstream of *WAKL11*. Intriguingly, *WAKL11* expression is associated with cell wall pectin metabolism. *WAKL11* knockout mutants displayed increased Cd sensitivity, whereas transgenic lines overexpressing *WAKL11* showed increased Cd tolerance (Figure S8A–D). Moreover, the overexpression of *WAKL11* in the *nac102* mutant brought the Cd sensitivity of these lines to almost the same level as that of WT plants (Figure 7A, B). The positive correlation between *WAKL11* expression and Cd

tolerance is consistent with the changes in cell wall pectin content, but not with the pattern of cell wall hemicellulose content (Figures 7C, S8E–G, S9). These results indicate that NAC102 affects cell wall pectin metabolism by regulating *WAKL11* expression.

VunAR1, a NAC TF from rice bean, has been demonstrated to regulate *VuWAK1* expression via directly binding to its promoter (Lou et al., 2019). Similarly, we determined here that in *Arabidopsis*, NAC102 regulates *WAKL11* transcription, as evidenced by the finding that NAC102 binds to the *WAKL11* promoter in EMSA and ChIP-qPCR (Figure 6B–F). Moreover, members of the WAK/WAKL family have previously been shown to be transcriptionally responsive to metal exposure. For example, *WAK1* is an early Al-responsive gene, and its overexpression confers aluminum (Al) tolerance to *Arabidopsis* seedlings (Sivaguru et al., 2003). *WAKL4* is transcriptionally activated by sodium (Na^+), potassium (K^+), copper (Cu^{2+}), nickel (Ni^{2+}), and zinc (Zn^{2+}) (Hou et al., 2005). Here, we established that *WAKL11* expression is induced by Cd stress (Figure 6A; Table S1). This implies that members of the *WAK/WAKL* gene family are transcriptionally regulated in response to various stresses, although the molecular mechanism of this regulation remains largely unknown. Insertion of a T-DNA in the *WAKL4* promoter (40 bp upstream its translational start codon) impaired transcriptional activation of this gene by Na^+, K^+, Cu^{2+}, and Zn^{2+}, but not by Ni^{2+} (Hou et al., 2005). However, which components are required for this induction is unknown. Our current finding, in combination with previous results by Lou et al. (2019), suggest that NAC TF family members function as upstream regulators of some *WAK/WAKL* family members.

It nevertheless remains unclear how WAKL11 regulates cell wall pectin metabolism. Lou et al. (2019) reported that *VuWAK1* transcript abundance was positively associated with the metabolism of pectin in cell walls. The *wak1* mutant had more pectin and transgenic lines overexpressing *WAK1* had less pectin compared to WT, with a negative correlation between pectin contents and Al accumulation in cell wall pectin fraction (Lou et al., 2019). WAK/WAKL family members contain cytoplasmic Ser/Thr kinase domains at their C termini and extracellular motifs at their N termini, including epidermal growth factor (EGF) repeats, EGF2-like domains, and Ca^{2+}-binding EGF domains (He et al., 1996, 1999; Verica and He, 2002). Experimental evidence suggested that WAKs bind covalently to cell wall pectin (Wagner and Kohorn, 2001). Therefore, it is possible that WAKL11 is closely associated with pectin, which would contribute to pectin metabolism, with the knockout of *WAKL11* leading to pectin accumulation in cell walls (Figure S8E).

Importantly, we observed a positive correlation between cell wall Cd content and Cd sensitivity in this study. In agreement with our findings, exogenous application of glucose or auxin improve Cd tolerance by increasing Cd fixation in the HC1 fraction of cell walls (Zhu et al., 2013; Shi et al., 2015). By contrast, phosphorus deficiency induced a decrease in pectin and hemicellulose polysaccharides, which was responsible for reduced cell wall fixation of Cd, contributing to the alleviation of Cd toxicity in *Arabidopsis* (Zhu et al., 2012). In rice, Cd induced the accumulation of the phytohormone gibberellic acid (GA), with GA regulating Cd tolerance by decreasing root cell wall Cd fixation (Liu et al., 2022). Therefore, the role of Cd fixation by cell walls in Cd tolerance remains controversial.

To explain these contradictory results, we propose the following model. Cd stress progressively affects plant growth. The root apoplast is the primary target site when roots are first exposed to Cd, and this is followed by the entry of Cd into the symplast. Therefore, it is reasonable that Cd stress would preferentially affect the root apoplast (Figure S2), resulting in the inhibition of root growth (Figure 1A–F) as well as water and nutrient uptake (He et al., 2017). Once Cd enters the symplast and is transported to leaves, it has direct effects on many metabolic pathways such as photosynthesis, thereby indirectly affecting shoot growth (Figure 1G). Therefore, from the perspective of progression of Cd toxicity, Cd adsorption to and within the cell wall will first lead to root damage. However, once the roots have acclimated to Cd toxicity through adjusting cell wall metabolism, the retention of Cd within cell walls will be beneficial, by limiting Cd transport to all cells and to the shoot. Moreover, Cd tolerance in plants requires coordination between roots and shoots, as well as between the apoplast and symplast. This notion is supported by a recent study in which NAC004 was shown to confer Cd tolerance by regulating Cd distribution and detoxification at various levels (Meng et al., 2022).

In summary, we demonstrate that Cd accumulation in root cell wall pectin contributes to the inhibition of root growth (Figure 7E). This toxic effect triggers a possible Cd stress signal that induces the expression of *NAC102.1*. Another possibility is that Cd binding to the cell wall results in pectin accumulation, which triggers *NAC102.1* induction. NAC102 then binds directly to the *WAKL11* promoter to activate transcription, which further contributes to cell wall pectin degradation, thereby decreasing Cd accumulation in roots and conferring Cd resistance.

MATERIALS AND METHODS

Plant materials and transgenic screening

The *Arabidopsis thaliana* Columbia (Col-0) accession was used as WT in the current work. The *Arabidopsis* mutant *nac102* (SALK_030702), a T-DNA insertion line in the Col-0 background, was obtained from the ABRC. Various transgenic plants were generated by *Agrobacterium tumefaciens*-mediated transformation via the standard floral-dip method (Lou et al., 2019).

The *35S:NAC102* construct was generated by cloning the full-length *NAC102.1* coding sequence (with stop codon) into a modified pCAMBIA1300 vector carrying the CaMV 35S promoter (35S::pCAMBIA1300), and then transformed into Col-0 to obtain *NAC102*-OE. A 2-kb promoter sequence

upstream of the *NAC102.1* translational start codon as well as its full coding region (without the stop codon) were amplified by PCR from Col-0 genomic DNA and cloned in-frame and upstream of the *GFP* sequence in the modified pCAMBIA1300 vector. The resulting *NAC102.1pro:NAC102.1-GFP* construct was transformed into *nac102* to generate COM lines. Two specific targets within the first exon of the *WAKL11* genomic sequence were selected, and the clone for CRISPR/Cas9-mediated genome editing was constructed as described by Zhang et al. (2017), before being introduced into Col-0 to produce *WAKL11*-knockout transgenic lines. The coding sequence of *WAKL11* with stop codon was cloned into the above 35S::pCAMBIA1300 vector, and the resulting plasmid was transformed into Col-0 to obtain the *WAKL11*-OE transgenic plants. Moreover, the *nac102 WAKL11*-OE lines and *nac102 wakl11* lines were produced by crossing *nac102* with *WAKL11*-OE or *wakl11*, respectively. Homozygous lines were obtained following self-pollination of F1 plants and confirmed by genomic PCR and Sanger sequencing. All gene-specific primers are listed in Table S2.

Growth conditions and Cd treatment

Arabidopsis seeds were surfaced sterilized and germinated on one-fifth-strength (1/5) Hoagland nutrient solution containing 1% (w/v) agar (Sigma-Aldrich). After 7 d, when the length of primary roots was approximately 1 cm, uniform seedlings were transferred to fresh plates containing 50 μmol/L $CdCl_2$ for 4 d, or allowed to grow hydroponically in aerated 1/5 Hoagland solution, which was refreshed every other day. The 1/5 Hoagland nutrient solution (pH 5.5) consisted of 1 mmol/L $Ca(NO_3)_2$, 1 mmol/L KNO_3, 400 μmol/L $MgSO_4$, 200 μmol/L $NH_4H_2PO_4$, 3 μmol/L H_3BO_3, 0.4 μmol/L $ZnSO_4$, 0.2 μmol/L $CuSO_4$, 0.5 μ $MnCl_2$, 1 μmol/L $(NH_4)_6(Mo_7)$, and 20 μmol/L Fe-ethylenediaminetetraacetic acid (EDTA).

To test tissue-specific expression during the early vegetative stage, 7-d-old seedlings were exposed to 1/5 Hoagland solution alone (normal conditions, −Cd) or with 30 μmol/L $CdCl_2$ (Cd stress conditions, +Cd) for 24 h. For tissue-specific expression during the reproductive stage, 7-d-old seedlings were grown in aerated, hydroponic 1/5 Hoagland solution for 5 weeks. In the time-course assays, 4-week-old plants were treated with 1/5 Hoagland solution containing 30 μmol/L Cd for 1, 3, 6, 9, 12, 24, 72, or 96 h. In the dose-response assays, 4-week-old plants were treated with 10, 30, 50, or 100 μmol/L $CdCl_2$ for 4 d, or maintained in 1/5 Hoagland solution lacking $CdCl_2$ as control. The solution was refreshed daily. All experiments were carried out in an environmentally controlled greenhouse with a 12-h light/12-h dark cycle at 22°C.

Phenotypic observations and Cd-specific fluorescence in roots

After a 4-d treatment under Cd stress, morphological changes of 7-d-old *Arabidopsis* seedlings (root length, root and shoot fresh weights) were evaluated and photographed with a Nikon digital camera. The distribution of Cd in roots was visualized by immersing the entire root into 0.04% (w/v) Leadmium Green staining solution (Molecular Probes, Invitrogen) based on a reported protocol (Lu et al., 2008) with minor modifications. After incubation at 25°C for 30 min in the dark, the signals of root Cd-specific fluorescence were recorded with a Nikon Eclipse Ni epifluorescence microscope with excitation at 488 nm and emission at 505 – 530 nm, with the laser intensity set to approximately 40% – 45% and the gain and offset adjustments among different genotypes kept constant. The relative fluorescence intensities were quantified by ImageJ software, and data are presented as the mean fluorescence intensity relative to that of Col-0 without Cd treatment.

Histochemical GUS staining assay

A *NAC102.1* promotor fragment (2,024 bp) was cloned upstream of the *GUS* reporter gene in pCAMBIA1300, and then transformed into Col-0. Homozygous lines carrying a single T-DNA copy were selected for GUS staining. Briefly, the entire seedlings or various dissected tissues (roots, leaves, buds, and siliques) were harvested from *NAC102.1pro::GUS* transgenic seedlings or plants, and incubated in 0.1 mol/L phosphate buffer (pH 7.0) containing 1 mg/mL X-gluc (Yeasen, China), 1 mmol/L $K_3Fe(CN)_6$, 1 mmol/L $K_4Fe(CN)_6$, 10 mmol/L EDTA, and 0.5% (v/v) Triton X-100. After incubation at 37°C overnight in darkness, chlorophyll was removed by incubation at 25°C in 70% (v/v) ethanol until the samples collected from the non-transformed Col-0 plants became clear. All samples were photographed with a VHX-6000 microscope (Keyence, Japan).

Similarly, the construct *WAKL11pro::GUS* (with a 1,001-bp *WAKL11* promoter fragment driving *GUS*) was generated, and then individually transformed into Col-0 and *nac102* to generate *WAKL11pro::GUS* and *nac102 WAKL11pro::GUS* reporter lines. Seven-d-old seedlings were maintained in control conditions (–Cd) or exposed to 30 μmol/L $CdCl_2$ for 24 h, histochemical staining for GUS activity was carried out in roots of transgenic lines as described above, and then the roots were photographed with a AZ100 stereoscope (Nikon, Japan).

RNA extraction and gene expression analysis

Total RNA was isolated from entire roots harvested from −Cd and +Cd-treated seedlings using an RNAprep Pure Plant Kit (Tiangen, China), and then subjected to DNase I digestion and reverse transcription using a FastKing RT Kit (Tiangen, China). End-point RT-PCR was performed on a S1000 machine (Bio-Rad, USA) using Taq master Mix from CWBIO, whereas RT-qPCR was performed on a Roche LightCycler480 machine using SYBR Green Mix from TOYOBO. The expression level of target genes was calculated and normalized against that of the internal reference *ACTIN2* as described (Chen et al., 2018). All primers are listed in Table S2.

Extraction, fractionation, and determination of cell wall components

Four-week-old seedlings were exposed to 30 μmol/L $CdCl_2$ (+Cd) for 4 d or maintained in control conditions (–Cd) before their roots were harvested. To remove surface Cd contamination, roots were rinsed in 1 mmol/L EDTA and then deionized water as described by Chen et al. (2018). Components of the root cell wall were extracted as previously described (Yang et al., 2011; Lou et al., 2019). Briefly, root samples were ground in liquid nitrogen, homogenized in 75% (v/v) ethanol, and then centrifuged to remove the supernatant. Afterwards, the pellets were washed sequentially with acetone, methanol:chloroform (1:1, v/v), and methanol. The final precipitates were freeze-dried and considered to represent crude cell walls. To fractionate cell wall components, about 5 mg of cell walls was incubated in boiling water three times for 1 h each time, and the supernatants were considered as pectin. The residue was extracted twice in 4% (w/v) KOH containing 0.02% (w/v) KBH_4 for 1 d, and then centrifuged; the supernatants were combined as HC1. The remaining sediments were further extracted twice in 24% (w/v) KOH containing 0.02% (w/v) KBH_4 for 1 d; the supernatant was collected following centrifugation and regarded as hemicellulose 2 (HC2). Finally, the final pellet was washed, dried, and collected as crude cellulose.

For the determination of cell wall components, uronic acid content was determined colorimetrically using GalUA (Sigma) as a standard (Blumenkrantz and Asboe-Hansen, 1973; Yang et al., 2011), with galacturonic acid equivalents used to indicate the relative amount of root pectin. Polysaccharide content was assayed colorimetrically using glucose (Sigma) as a standard (Dubois et al., 1956; Yang et al., 2011), with total sugar equivalents used to indicate the relative amount of HC1 or HC2. Finally, the crude cellulose extracts were dried and weighed to indicate root cellulose content.

Cd content measurement

For total Cd determination, according to Chen et al. (2018), roots and shoots were collected after a 4-d treatment under −Cd or +Cd conditions, and rinsed in 1 mmol/L EDTA and deionized water to remove Cd contamination on the surface of plant materials. Subsequently, root and shoot samples were oven-dried, weighed, and digested with concentrated HNO_3 for the measurement of Cd contents by ICP-OES (AIRIS/AP, TJA, ThermoFisher Scientific).

For Cd determination in the root symplast and apoplast, 4-week-old plants were subjected to 30 μmol/L $CdCl_2$ for 4 d or maintained in Cd-free conditions, in which roots were collected at 24-h intervals. After washes with 1 mmol/L EDTA and distilled water to remove surface contamination by Cd following the protocol by Chen et al. (2018), fresh roots were weighed, frozen at –80°C, and then thawed to room temperature. The samples were centrifuged in Millipore centrifugal filters to obtain the symplastic solution and the apoplast, as previously described (Lou et al., 2019). After digestion with concentrated HNO_3, the Cd concentration was detected by ICP-OES as above.

For Cd determination in the cell wall fractions according to Shi et al. (2015), 2 mol/L HCl was used to extract Cd from the pectin, HC1 and HC2 fractions. After incubation for 24 h with occasional shaking, the Cd concentration was measured by ICP-OES.

Localization and abundance of NAC102-GFP

To examine whether the abundance of NAC102 protein changes under Cd stress, 7-d-old seedlings from COM lines harboring the *NAC102.1pro:NAC102.1-GFP* transgene were transferred from –Cd medium to +Cd medium for 10 min, and then the roots were observed and GFP fluorescence was captured using an LSM710 confocal laser-scanning microscope (Karl Zeiss, Germany).

To visualize the subcellular localization of NAC102 via confocal microscopy, the construct *35S::NAC102.1-GFP* was generated by cloning the full-length *NAC102.1* coding sequence without the stop codon into the modified vector 35S::pCAMBIA1300-GFP with gene-specific primers (Table S2). For transient expression assays according to Zhu et al. (2022), the construct together with *H2B-RFP* (Martin et al., 2009), a construct encoding the nucleus marker histone H2B fused to RFP, were co-infiltrated into the leaves of 4-week-old *Nicotiana benthamiana*. After 48 h, the fluorescence signals were observed. The same *35S::NAC102.1-GFP* construct was introduced into Col-0 plants; homozygous T3 lines, named *35S::NAC102-GFP*, were selected for GFP analysis, with DAPI (DNA-4′,6-diamidino-2-phenylindole complex) staining serving to label the nuclei.

Transactivation assays

To explore the transactivation potential of NAC102 in yeast, the full length or fragments of the *NAC102.1* coding sequence were PCR-amplified with gene-specific primers (Table S2), and then individually cloned into the vector pGBKT7. Each recombinant plasmid was introduced into yeast (*Saccharomyces cerevisiae*) strain AH109 according to the Matchmaker Gold System (Clontech) and then cultured for 3 d on SD medium with or without histidine (His) at 30°C. Yeast cells carrying the empty pGBKT7 vector served as the negative control.

Protein-DNA interaction assays

For yeast one-hybrid assays (Y1Hs), various *WAKL11* promoter fragments were separately cloned into the vector pAbAi, whereas the full-length *NAC102.1* coding sequence was inserted into the vector pGADT7. Primers are listed in Table S2. Plasmid pairs of pAbAi-*WAKL11pro* and pGADT7-*NAC102.1* were transformed into yeast strain *Y1HGold* according to the instructions provided by Clontech, and then grown at 30°C for 3 d on SD medium lacking Ura or lacking Ura and containing 200 ng/mL aureobasidin A (AbAi).

For ChIP-qPCR assays, 4-week-old COM (*nac102 NAC102.1pro::NAC102.1-GFP*) transgenic lines and Col-0 plants were treated with +Cd medium for 24 h, then roots were collected and cross-linked with 1% (w/v) formaldehyde. The ChIP assay was conducted with an EpiQuik Plant ChIP Kit (Epigentek, USA), in which chromatin DNA was isolated, sonicated, and then

immunoprecipitated with anti-GFP antibody (Abcam, England). Afterwards, the precipitated DNA was eluted, purified, and then subjected to qPCR as described by Xu et al. (2019). The gene-specific primers (Table S2) were designed to amplify *WAKL11* promoter fragments A1, A5, A6, and A7. The relative ChIP enrichment was evaluated by normalizing the immunoprecipitation efficiency of transgenic plants to that of Col-0 plants.

For dual-LUC assays, the promoter fragments A1, A5, A6, and A7 of *WAKL11* were PCR-amplified using specific primers (Table S2) and then separately inserted into pGreenII0800-LUC (with the firefly luciferase gene, *LUC*, driven by a 35Smini promoter; Hellens et al., 2005) as a reporter, with *35S::NAC102.1* described used as effector construct. The leaves of 4-week-old *N. benthamiana* plants were co-infiltrated with mixtures of *Agrobacterium* (strain GV3101) colonies harboring the reporter or the effector construct. At 48 h post-infiltration, LUC activity was measured and quantified using a NightShade LB985 instrument (Berthold, Germany), as described by Chen et al. (2018). The empty vectors pGreenII0800-LUC and pCAMBIA1300 were used as negative controls.

For *in vitro* gel-shift assays, according to Zhu et al. (2022), NAC102 was purified from 4-week-old *Arabidopsis* plants harboring the *35S::NAC102-GFP* transgene with a commercial anti-GFP antibody (ABclonal Technology), whereas double-stranded DNA probes and competitors were amplified by PCR using biotin-labeled or unlabeled primers (Table S2). Subsequently, an EMSA was performed with a Chemiluminescent EMSA Kit (Beyotime Biotechnology).

Statistical analysis

For all assays, quantitative data are reported as means ± *SD*, generated from at least three biological replicates in repeated experiments. Tukey's test in a one-way analysis of variance procedure was performed to analyze whether there were statistically significant differences at the level of $P \leq 0.05$ among various genotypes under −Cd or +Cd treatment.

Data availability statement

Supporting data for this work are available within the paper and its online supplementary information. All *Arabidopsis* materials, including Col-0, the *nac102* mutant and numerous transgenic lines obtained in the Col-0 or *nac102* background, are available in our lab.

ACKNOWLEDGEMENTS

This work was financially supported by grants from the National Natural Science Foundation of China (32270215, 31601765), the Natural Science Foundation of Zhejiang Province (LY19C150006), the China Postdoctoral Science Foundation (2019M652064), the China Scholarship Council (2016)3035), and the Hangzhou Innovation Project for Returned Chinese Scholars.

CONFLICTS OF INTEREST

The authors declare no conflicts of interest.

AUTHOR CONTRIBUTIONS

G.H.H. and R.N.H. performed the experiments, analyzed the data, and helped write the original draft. L.H.H. and J.X.X. participated in material preparation and data analysis. Y.G.H. was involved in technical assistance and manuscript editing. Y.H.W. and W.W.C. initiated and conceived the project, analyzed the data, and wrote the manuscript. All authors read and approved the manuscript.

Edited by: Zhaojun Ding, Shandong University, China

Received Apr. 22, 2023; **Accepted** Aug. 10, 2023; **Published** Aug. 11, 2023

REFERENCES

Blumenkrantz, N., and Asboe-Hansen, G. (1973). New method for quantitative determination of uronic acids. Anal. Biochem. **54:** 484–489.

Chen, J., Yang, L.B., Yan, X.X., Liu, Y.L., Wang, R., Fan, T.T., Ren, Y.B., Tang, X.F., Xiao, F.M., Liu, Y.S., et al. (2016). Zinc-finger transcription factor ZAT6 positively regulates cadmium tolerance through the glutathione-dependent pathway in Arabidopsis. Plant Physiol. **171:** 707–719.

Chen, W.W., Jin, J.F., Lou, H.Q., Liu, L., Kochian, L.V., and Yang, J.L. (2018). LeSPL-CNR negatively regulates Cd acquisition through repressing nitrate reductase-mediated nitric oxide production in tomato. Planta **248:** 893–907.

Christianson, J.A., Wilson, I.W., Llewellyn, D.J., and Dennis, E.S. (2009). The low-oxygen-induced NAC domain transcription factor ANAC102 affects viability of Arabidopsis seeds following low-oxygen treatment. Plant Physiol. **149:** 1724–1738.

Clemens, S., Aarts, M.G.M., Thomine, S., and Verbruggen, N. (2013). Plant science: the key to preventing slow cadmium poisoning. Trends Plant Sci. **18:** 92–99.

D'Alessandro, S., Ksas, B., and Havaux, M. (2018). Decoding β-cyclocitral-mediated retrograde signaling reveals the role of a detoxification response in plant tolerance to photooxidative stress. Plant Cell **30:** 2495–2511.

Du, X.Y., He, F., Zhu, B., Ren, M.J., and Tang, H. (2020). NAC transcription factors from *Aegilops markgrafii* reduce cadmium concentration in transgenic wheat. Plant Soil. **449:** 39–50.

Dubois, M., Gilles, K.A., Hamilton, J.K., Rebers, P.A., and Smith, F. (1956). Colori metric method for determination of sugars and related substances. Anal. Chem. **28:** 350–356.

Hall, J.L. (2002). Cellular mechanisms for heavy metal detoxification and tolerance. J. Exp. Bot. **53:** 1–11.

He, S., Yang, X., He, Z., and Baligar, V.C. (2017). Morphological and physiological responses of plants to cadmium toxicity: A review. Pedosphere **27:** 421–438.

He, Z.H., Cheeseman, I., He, D., and Kohorn, B.D. (1999). A cluster of five cell wall-associated receptor kinase genes, *Wak1-5*, are expressed in specific organs of Arabidopsis. Plant Mol. Biol. **39:** 1189–1196.

He, Z.H., Fujiki, M., and Kohorn, B.D. (1996). A cell wall-associated, receptor-like protein kinase. J. Biol. Chem. **271:** 19789–19793.

Hellens, R.P., Allan, A.C., Friel, E.N., Bolitho, K., Grafton, K., Templeton, M.D., Karunairetnam, S., and Laing, W.A. (2005). Transient expression vectors for functional genomics, quantification of promoter activity and RNA silencing in plants. Plant Methods **1:** 13.

Hou, X.W., Tong, H.Y., Selby, J., DeWitt, J., Peng, X.X., and He, Z.H. (2005). Involvement of a cell wall-associated kinase, WAKL4, in Arabidopsis mineral responses. Plant Physiol. **139:** 1704–1716.

Hu, S.B., Shinwari, K.I., Song, Y.X.R., Xia, J.X., Xu, H., Du, B.B., Luo, L., and Zheng, L.Q. (2021). OsNAC300 positively regulates cadmium stress responses and tolerance in rice roots. Agronomy. **11:** 95.

Jin, J.F., Zhu, H.H., He, Q.Y., Li, P.F., Fan, Wei, Xu, J.M., Yang, J.L., and Chen, W.W. (2022). The tomato transcription factor SlNAC063 is required for aluminum tolerance by regulating SlAAE3-1 expression. Front. Plant Sci. **12:** 826954.

Kochian, L.V. (1995). Cellular mechanisms of aluminum toxicity and resistance in plants. Annu. Rev. Plant Physiol. Plant Mol. Biol. **46:** 237–260.

Kong, X.P., Liu, G.C., Liu, J.J., and Ding, Z.J. (2018). The root transition zone: A hot spot for signal crosstalk. Trends Plant Sci. **23:** 403–409.

Liu, Y.S., Tao, Y., Yang, X.Z., Liu, Y.N., Shen, R.F., and Zhu, X.F. (2022). Gibberellic acid alleviates cadmium toxicity in rice by regulating NO accumulation and cell wall fixation capacity of cadmium. J. Hazar. Mater. **439:** 129597.

Lou, H.Q., Fan, W., Jin, J.F., Xu, J.M., Chen, W.W., Yang, J.L., and Zheng, S.J. (2019). A NAC-type transcription factor confers aluminium resistance by regulating cell wall-associated receptor kinase 1 and cell wall pectin. Plant Cell Environ. **43:** 463–478.

Lu, L.L., Tian, S.K., Yang, X.E., Wang, X.C., Brown, P., Li, T.Q., and He, Z.L. (2008). Enhanced root-to-shoot translocation of cadmium in the hyperaccumulating ecotype of *Sedum alfredii*. J. Exp. Bot. **59:** 3203–3213.

Lux, A., Martinka, M., Vaculík, M., and White, J.P. (2011). Root responses to cadmium in the rhizosphere: a review. J. Exp. Bot. **62:** 21–37.

Martin, K., Kopperud, K., Chakrabarty, R., Banerjee, R., Brooks, R., and Goodin, M.M. (2009). Transient expression in *Nicotiana benthamiana* fluorescent marker lines provides enhanced definition of protein localization, movement and interactions in planta. Plant J. **59:** 150–162.

Meng, Y.T., Zhang, X.L., Wu, Q., Shen, R.F., and Zhu, X.F. (2022). Transcription factor ANAC004 enhances Cd tolerance in *Arabidopsis thaliana* by regulating cell wall fixation, translocation and vacuolar detoxification of Cd, ABA accumulation and antioxidant capacity. J. Hazar. Mater. **436:** 129121.

Parrotta, L., Guerriero, G., Sergeant, K., Cai, G., and Hausman, J.F. (2015). Target or barrier? The cell wall of early- and later-diverging plants vs cadmium toxicity: differences in the response mechanisms. Front. Plant Sci. **6:** 133.

Peng, H., and Neff, M.M. (2021). Two ATAF transcription factors ANAC102 and ATAF1 contribute to the suppression of cytochrome P450-mediated brassinosteroid catabolism in Arabidopsis. Physiol. Plant. **172:** 1493–1505.

Puranik, S., Sahu, P.P., Srivastava, P.S., and Prasad, M. (2012). NAC proteins: regulation and role in stress tolerance. Trend Plant Sci. **17:** 369–381.

Shahid, M., Dumat, C., Khalid, S., Niazi, N.K., and Antunes, P.M.C. (2017). Cadmium bioavailability, uptake, toxicity and detoxification in soil-plant system. Rev. Environ. Contam. Toxicol. **241:** 73–137.

Sheng, Y.B., Yan, X.X., Huang, Y., Yan, Y.Y., Zhang, C., Ren, Y.B., Fan, T.T., Xiao, F.M., Liu, Y.S., and Cao, S.Q. (2019). The WRKY transcription factor, WRKY13, activates PDR8 expression to positively regulate cadmium tolerance in Arabidopsis. Plant Cell Environ. **42:** 891–903.

Shi, Y.Z., Zhu, X.F., Wan, J.X., Li, G.X., and Zheng, S.J. (2015). Glucose alleviates cadmium toxicity by increasing cadmium fixation in root cell wall and sequestration into vacuole in Arabidopsis. J. Integr. Plant Biol. **57:** 830–837.

Shim, D., Hwang, J., Lee, J., Lee, S., Choi, Y., An, G., Martinoia, E., and Lee, Y. (2009). Orthologs of the class A4 heat shock transcription factor HsfA4a confer cadmium tolerance in wheat and rice. Plant Cell **21:** 4031–4043.

Simpson, S.D., Nakashima, K., Narusaka, Y., Seki, M., Shinozaki, K., and Yamaguchi-Shinozaki, K. (2003). Two different novel cis acting elements of erd1, a clpA homologous Arabidopsis gene function in induction by dehydration stress and dark-induced senescence. Plant J. **33:** 259–270.

Sivaguru, M., Ezaki, B., He, Z.H., Tong, H., Osawa, H., Baluska, F., Volkmann, D., and Matsumoto, H. (2003). Aluminum induced gene-expression and protein localization of a cell wall-associated receptor protein kinase in Arabidopsis. Plant Physiol. **132:** 2256–2266.

Somerville, C., Bauer, S., Brininstool, G., Facette, M., Hamann, T., Milne, J., Osborne, E., Paredez, A., Persson, S., Raab, T., et al. (2004). Toward a systems approach to understanding plant cell walls. Science **306:** 2206–2211.

Tran, L.S.P., Nakashima, K., Sakuma, Y., Simpson, S.D., Fujita, Y., Maruyama, K., Fujita, M., Seki, M., Shinozaki, K., and Yamaguchi-Shinozaki, K. (2004). Isolation and functional analysis of Arabidopsis stress-inducible NAC transcription factors that bind to a drought responsive cis-element in the early responsive to dehydration stress 1 promoter. Plant Cell **16:** 2481–2498.

Verica, J.A., and He, Z.H. (2002). The cell wall-associated kinase (WAK) and WAK-like kinase gene family. Plant Physiol. **129:** 455–459.

Wagner, T., and Kohorn, B. (2001). Wall-associated kinases are expressed throughout plant development and are required for cell expansion. Plant Cell **13:** 303–318.

Wang, B.X., Zhang, M.M., Zhang, J., Huang, L.P., Chen, X., Jiang, M.Y., and Tan, M.P. (2020). Profiling of rice Cd-tolerant genes through yeast-based cDNA library survival screening. Plant Physiol. Biochem. **155:** 429–436.

Wang, C.Y., Qiao, F., Wang, M.Q., Wang, Y., Xu, Y., and Qi, X.T. (2023). PvERF104 confers cadmium tolerance in Arabidopsis: Evidence for metal-responsive element-binding transcription factors. Environ. Exp. Bot. **206:** 105167.

Willats, W.G.T., Knox, P., and Mikkelsen, J.D. (2006). Pectin: New insights into an old polymer are starting to gel. Trends Food Sci. Technol. **17:** 97–104.

Wu, H.L., Chen, C.L., Du, J., Liu, H.F., Cui, Y., Zhang, Y., He, Y.J., Wang, Y.Q., Chu, C.C., Feng, Z.Y., et al. (2012). Co-overexpression FIT with AtbHLH38 or AtbHLH39 in Arabidopsis-enhanced cadmium tolerance via increased cadmium sequestration in roots and improved iron homeostasis of shoots. Plant Physiol. **158:** 790–800.

Xu, J.M., Wang, Z.Q., Wang, J.Y., Li, P.F., Jin, J.F., Chen, W.W., Fan, W., Kochain, L.V., Zheng, S.J., and Yang, J.L. (2019). Low phosphate represses histone deacetylase complex1 to regulate root system architecture remodeling in Arabidopsis. New Phytol. **225:** 1732–1745.

Yang, J.L., Li, Y.Y., Zhang, Y.J., Zhang, S.S., Wu, Y.R., Wu, P., and Zheng, S.J. (2008). Cell wall polysaccharides are specifically involved in the exclusion of aluminum from the rice root apex. Plant Physiol. **146:** 602–611.

Yang, J.L., Zhu, X.F., Peng, X.Y., Zheng, C., Li, G.X., Liu, Y., Shi, Y.Z., and Zheng, S.J. (2011). Cell wall hemicellulose contributes significantly to aluminum adsorption and root growth in Arabidopsis. Plant Physiol. **155:** 1885–1892.

Zhang, H.Y., Wang, X.H., Dong, L., Wang, Z.P., Liu, B., Lv, J., Xing, H. L., Han, C.Y., Wang, X.C., and Chen, Q.J. (2017). MISSA 2.0: An updated synthetic biology toolbox for assembly of orthogonal CRISPR/Cas systems. Sci. Rep. **7:** 41993.

Zhang, P., Wang, R.L., Ju, Q., Li, W.Q., Tran, L.S.P., and Xu, J. (2019). The R2R3-MYB transcription factor MYB49 regulates cadmium accumulation. Plant Physiol. **180:** 529–542.

Zhang, Q., Cai, W., Ji, T.T., Ye, L., Lu, Y.T., and Yuan, T.T. (2020). WRKY13 enhances cadmium tolerance by promoting *D-CYSTEINE DESULFHYDRASE* and hydrogen sulfide production. Plant Physiol. **183:** 345–357.

Zhu, H.H., Wang, J.Y., Jiang, D., Hong, Y.G., Xu, J.M., Zheng, S.J., Yang, J.L., and Chen, W.W. (2022). The miR157-SPL-CNR module acts upstream of bHLH101 to negatively regulate iron deficiency responses in tomato. J. Integr. Plant Biol. **64:** 1059–1075.

Zhu, X.F., Lei, G.J., Jiang, T., Liu, Y., Li, G.X., and Zheng, S.J. (2012). Cell wall polysaccharides are involved in P-deficiency-induced Cd exclusion in *Arabidopsis thaliana*. Planta **236:** 989–997.

Zhu, X.F., Wang, Z.W., Dong, F., Lei, G.J., Shi, Y.Z., Li, G.X., and Zheng, S.J. (2013). Exogenous auxin alleviates cadmium toxicity in *Arabidopsis thaliana* by stimulating synthesis of hemicellulose 1 and increasing the cadmium fixation capacity of root cell walls. J. Hazar. Mater. **263:** 398–403.

SUPPORTING INFORMATION

Additional Supporting Information may be found online in the supporting information tab for this article: http://onlinelibrary.wiley.com/doi/10.1111/jipb.13557/suppinfo

Figure S1. Construction of NAC102.1-related *Arabidopsis* transgenic lines

Figure S2. Time-course response of cadmium (Cd) stress to root symplasmic and apoplastic Cd deposit

Figure S3. Cellulose content and its cadmium (Cd) accumulation in response to Cd stress

Figure S4. Root pectin accumulation is related to cadmium (Cd) concentrations in *Arabidopsis*

Figure S5. Tissue-specific expression pattern of *NAC102.1* in *Arabidopsis*

Figure S6. The expression pattern of *NAC102.1* in *Arabidopsis* roots in response to cadmium (Cd) stress

Figure S7. Immunoblot analysis of NAC102 protein

Figure S8. The participation of WALL-ASSOCIATED KINASE-LIKE PROTEIN11 (WAKL11) in cadmium (Cd) tolerance

Figure S9. Cell wall hemicelluloses are not involved in WALL-ASSOCIATED KINASE-LIKE PROTEIN11 (WAKL11)-mediated cadmium (Cd) sensitivity of mutant *nac102*

Table S1. Differential expression analysis revealed the probable participation of *WALL-ASSOCIATED KINASE-LIKE PROTEIN11* (*WAKL11*) in *NAC102.1*-mediated cadmium (Cd) resistance

Table S2. Primers used in this study